

Supplemental information

**MultiEditR: The first tool for the detection and
quantification of RNA editing from Sanger sequencing
demonstrates comparable fidelity to RNA-seq**

Mitchell G. Kluesner, Rafail Nikolaos Tasakis, Taga Lerner, Annette Arnold, Sandra Wüst, Marco Binder, Beau R. Webber, Branden S. Moriarity, and Riccardo Pecori

SUPPLEMENTARY MATERIALS

pJET-CmAG-WT and pJET-CmAG-6x

CTCCCACAACGAGGACTACACCATCGTGGAACAGTACGAACGCGCCGAGGGCCGCC
ACTCCACCGGCGGCATGGACGAGCTGTACAAGaagcttaAACAAGTAGCTGGTGCCAAG
GAAAAAATAACTTCTTTCATGGAAAATTATAGAATTACAGATAATGATGTACTAATT
GCCATAGATAGTGCCAAAATCAACTTCAATGAAAAA**C**TCTCTCAA**C**TTGAGACATA
CGCGATA**C**AATTTGATCAGTATATTAAGATAATTATGATCCACATGAC**C**TTAAAAAG
AA**C**TATTGCTGAGATTATTGAT**C**GAATCATTGAAAAGTTAAAAATTCTTGATGAACA
GTATCATATCCGTGTAAATCTAGCAAAATCAATCCATAATCTCTATTTATTTGTTGAA
AACGTTGATCTTAACCAAGTCAGTAGTAGTAACACCTCTTGGATCCAAAATGTGGAT
TCCAATTATCAAGTCAGAATCCAAATTCAAGAAAACTACAGCAGCTCAGGACACA
AATTCAGAATATAGACATTCAGCAGCTTGCTGCAGAGGTAAAACGACAG

In **yellow** are highlighted the 6 Cs which are unedited (C) in pJET-CmAG-WT and edited (T) in the pJET-CmAG-6x.

mCherry-mApoB-eGFP (CmAG) coding region:

ATGGTGAGCAAGGGCGAGGAGGATAACATGGCCATCATCAAGGAGTTCATGCGCTT
CAAGGTGCACATGGAGGGCTCCGTGAACGGCCACGAGTTCGAGATCGAGGGCGAGG
GCGAGGGCCGCCCTACGAGGGCACCCAGACCGCCAAGCTGAAGGTGACCAAGGGT
GGCCCCCTGCCCTTCGCCTGGGACATCCTGTCCCCTCAGTTCATGTACGGCTCCAAG
GCCTACGTGAAGCACCCCGCCGACATCCCCGACTACTTGAAGCTGTCCTTCCCCGAG
GGCTTCAAGTGGGAGCGCGTGATGAACTTCGAGGACGGCGGCGTGGTGACCGTGAC
CCAGGACTCCTCCCTGCAGGACGGCGAGTTCATCTACAAGGTGAAGCTGCGCGGCA
CCAACTTCCCCTCCGACGGCCCCGTAATGCAGAAGAAGACCATGGGCTGGGAGGCC
TCCTCCGAGCGGATGTACCCCGAGGACGGCGCCCTGAAGGGCGAGATCAAGCAGAG
GCTGAAGCTGAAGGACGGCGGCCACTACGACGCTGAGGTCAAGACCACCTACAAGG
CCAAGAAGCCCGTGCAGCTGCCCGGCGCCTACAACGTCAACATCAAGTTGGACATC
ACCTCCCACAACGAGGACTACACCATCGTGGAACAGTACGAACGCGCCGAGGGCCG
CCACTCCACCGGCGGCATGGACGAGCTGTACAAGaagcttaAACAAGTAGCTGGTGCCA
AGGAAAAAATAACTTCTTTCATGGAAAATTATAGAATTACAGATAATGATGTACTAA
TTGCCATAGATAGTGCCAAAATCAACTTCAATGAAAAACTCTCTCAACTTGAGACAT
ACGCGATACAATTTGATCAGTATATTAAGATAATTATGATCCACATGACTTAAAAA
GAACTATTGCTGAGATTATTGATCGAATCATTGAAAAGTTAAAAATTCTTGATGAAC
AGTATCATATCCGTGTAAATCTAGCAAAATCAATCCATAATCTCTATTTATTTGTTGA
AAACGTTGATCTTAACCAAGTCAGTAGTAGTAACACCTCTTGGATCCAAAATGTGGA

TTCCAATTATCAAGTCAGAATCCAAATTCAAGAAAACTACAGCAGCTCAGGACAC
AAATTCAGAATATAGACATTCAGCAGCTTGCTGCAGAGGTAAAACGACAGACCCGG
GATCCACCGGTGCGCCACCATGGTGAGCAAGGGCGAGGAGCTGTTACCGGGGTGGT
GCCATCCTGGTCGAGCTGGACGGCGACGTAAACGGCCACAAGTTCAGCGTGTCCG
GCGAGGGCGAGGGCGATGCCACCTACGGCAAGCTGACCCTGAAGTTCATCTGCACC
ACCGGCAAGCTGCCCCTGCCCTGGCCCACCCTCGTGACCACCCTGACCTACGGCGTG
CAGTGCTTCAGCCGCTACCCCGACCACATGAAGCAGCACGACTTCTTCAAGTCCGCC
ATGCCCCGAAGGCTACGTCCAGGAGCGCACCATCTTCTTCAAGGACGACGGCAACTA
CAAGACCCGCGCCGAGGTGAAGTTCGAGGGCGACACCCTGGTGAACCGCATCGAGC
TGAAGGGCATCGACTTCAAGGAGGACGGCAACATCCTGGGGCACAAGCTGGAGTAC
AACTACAACAGCCACAACGTCTATATCATGGCCGACAAGCAGAAGAACGGCATCAA
GGTGAACTTCAAGATCCGCCACAACATCGAGGACGGCAGCGTGCAGCTCGCCGACC
ACTACCAGCAGAACCCCCATCGGCGACGGCCCCGTGCTGCTGCCCGACAACCAC
TACCTGAGCACCCAGTCCGCCCTGAGCAAAGACCCCAACGAGAAGCGCGATCACAT
GGTCCTGCTGGAGTTCGTGACCGCCGCCGGGATCACTCTCGGCATGGACGAGCTGTA
CAAGTAA

In red mCherry, in yellow mouse Apob and in green eGFP.

mCherry-Apob-eGFP W58X (CAGX) coding region:

ATGGTGAGCAAGGGCGAGGAGGATAACATGGCCATCATCAAGGAGTTCATGCGCTT
CAAGGTGCACATGGAGGGCTCCGTGAACGGCCACGAGTTCGAGATCGAGGGCGAGG
GCGAGGGCCGCCCTACGAGGGCACCCAGACCGCCAAGCTGAAGGTGACCAAGGGT
GGCCCCCTGCCCTTCGCCTGGGACATCCTGTCCCCTCAGTTCATGTACGGCTCCAAG
GCCTACGTGAAGCACCCCGCCGACATCCCCGACTACTTGAAGCTGTCCTTCCCCGAG
GGCTTCAAGTGGGAGCGCGTGATGAACTTCGAGGACGGCGGGCGTGGTGACCGTGAC
CCAGGACTCCTCCCTGCAGGACGGCGAGTTCATCTACAAGGTGAAGCTGCGCGGCA
CCAACTTCCCCTCCGACGGCCCCGTAATGCAGAAGAAGACCATGGGCTGGGAGGCC
TCCTCCGAGCGGATGTACCCCGAGGACGGCGCCCTGAAGGGCGAGATCAAGCAGAG
GCTGAAGCTGAAGGACGGCGGCCACTACGACGCTGAGGTCAAGACCACCTACAAGG
CCAAGAAGCCCGTGCAGCTGCCCGGCGCCTACAACGTCAACATCAAGTTGGACATC
ACCTCCCACAACGAGGACTACACCATCGTGGAACAGTACGAACGCGCCGAGGGCCG
CCACTCCACCGGCGGCATGGACGAGCTGTACAAGAAGCTTACCATGGCCAAGGAGA
AACTGACTGCTCTCACAAAAAAGTATAGAATTACAGAAAATGATATACAAATTGCA
TTAGATGATGCCAAAATCAACTTTAATGAAAACTATCTCAACTGCAGACATATATG
ATACAATTTGATCAGTATATTAAAGATAGTTATGATTTACATGATTTGAAAATAGCT
ATTGCTAATATTATTGATGAAATCATTGAAAAATTA AAAAGTCTTGATGAGCACTAT
CATATCCGTGTA AATTTAGTAAAAACAATCCATGATCTACATTTGTTTATTGAAAAT
ATTGATTTTAACAAAAGTGGAAGTAGTACTGCATCCTGGATTCAAAAATGTGGATACT

AAGTACCAAATCAGAATCCAGATACAAGAAAACTGCAGCAGCTTAAGAGACACAT
ACAGAATATAGACATCCAGCACCTAGCTGGAATTCTGCAGTCGACGGTACCGCGGG
CCCGGGATCCACCGGTCGCCACCATGGTGAGCAAGGGCGAGGAGCTGTTACCGGG
GTGGTGCCCATCCTGGTCGAGCTGGACGGCGACGTAAACGGCCACAAGTTCAGCGT
GTCCGGCGAGGGCGAGGGCGATGCCACCTACGGCAAGCTGACCCTGAAGTTCATCT
GCACCACCGGCAAGCTGCCCGTGCCCTAGGCCACCCTCGTGACCACCCTGACCTACG
GCGTGCAGTGCTTCAGCCGCTACCCCGACCACATGAAGCAGCACGACTTCTTCAAGT
CCGCCATGCCC GAAGGCTACGTCCAGGAGCGCACCATCTTCTTCAAGGACGACGGC
AACTACAAGACCCGCGCCGAGGTGAAGTTCGAGGGCGACACCCTGGTGAACCGCAT
CGAGCTGAAGGGCATCGACTTCAAGGAGGACGGCAACATCCTGGGGCACAAGCTGG
AGTACA ACTACAACAGCCACAACGTCTATATCATGGCCGACAAGCAGAAGAACGGC
ATCAAGGTGAACTTCAAGATCCGCCACAACATCGAGGACGGCAGCGTGCAGCTCGC
CGACCACTACCAGCAGAACACCCCATCGGCGACGGCCCCGTGCTGCTGCCCGACA
ACCACTACCTGAGCACCCAGTCCGCCCTGAGCAAAGACCCCAACGAGAAGCGCGAT
CACATGGTCCTGCTGGAGTTCGTGACCGCCGCCGGGATCACTCTCGGCATGGACGAG
CTGTACAAGTAA

In red mCherry, in yellow human Apob and in green eGFP. In light blue is highlighted W58X mutation and in red the A to edit to G to re-activate the eGFP.

SUPPLEMENTARY TABLES

Supplementary Table 1 - List of all the regions within transcripts analysed with REDIttools v1 for NGS comparison with MultiEditR. For each transcript strandness, reference genome and chromosomal coordinates of the amplicon are indicated.

Gene (strand)	Reference Genome	Chromosomal coordinates of the amplicon
ARSD (reg.1) (-)	hg19	chrX:2,824,741-2,825,282
ARSD (reg.2) (-)	hg19	chrX:2,824,114-2,824,494
CTSS (-)	hg19	chr1:150,704,237-150,704,783
DDX58 (-)	hg19	chr9:32,455,300-32,502,734
MAVS (+)	hg19	chr20:3,827,446-3,856,770
SSR3 (-)	hg19	chr3:156,257,929-156,272,973
Slc39a10 (-)	mm10	chr1:46,807,710-46,808,199
Aldoc (+)	mm10	chr11:78,327,206-78,327,625
Atp6ap2 (+)	mm10	chrX:12,615,885-12,616,656
Serinc1 (-)	mm10	chr10:57,515,845-57,516,141
B2m (+)	mm10	chr2:122,147,686-122,153,083
Rab7 (-)	mm10	chr6:87,999,398-87,999,968
Reep5 (-)	mm10	chr18:34,346,596-34,347,035
Casp6 (+)	mm10	chr3:129,913,560-129,914,011

Supplementary Table 2 - List of all the regions within transcripts analysed by Amplicon-seq.
 For each transcript strandness, reference genome and chromosomal coordinates of the amplicon are indicated.

Gene (strand)	Reference Genome	Chromosomal coordinates of the amplicon
ARSD (-)	hg19	chrX:2824741-2825282
CTSS (-)	hg19	chr1:150704237-150704783
DDX58 (-)	hg19	chr9:32456205-32456648
MAVS (+)	hg19	chr20:3851441-3851945
Slc39a10 (-)	mm10	chr1:46807710-46808199
Aldoc (+)	mm10	chr11:78327206-78327625
Atp6ap2 (+)	mm10	chrX:12616190-12616656
Serinc1 (-)	mm10	chr10:57515845-57516325
B2m (+)	mm10	chr2:122152650-122153068
Rab7 (-)	mm10	chr6:87999398-87999968

Supplementary Table 3 - List of all the primers and oligos used in this study. For all the primers and oligos listed above lowercase bases represent the homology part needed during the cloning (#1-8, 17) or the adaptor sequence needed for Amplicon-seq (#57-76). For oligos #13-14 the base in bold is the one modified during the site-directed mutagenesis. In oligo #17 gRNA the bases highlighted in green codify the boxB hairpin. Oligos #27-56 were used to generate the PCR fragments used in the comparison of MultiEditR and NGS methods (Figure 2 and S4).

1	mApob_F	ggcggcatggacgagctgtacaagAAGCTTAAACAAGTAGCTGGTGCCAAGGAA
2	mApob_R	accatggtggcgaccggtggatccccgggCTGTTCGTTTTACCTCTGCAGCAAG
3	RBM47_F	ttagtgaaccgtcagatccgctagcATGACTGCTGAAGATTCCGCC
4	RBM47_R	agagtgcggccgcttactgtacaTCAGTAAGTCTGGTAGACGTCG
5	CRISPR sgRNA ADAR1ko_ exon4_F	caccGGACAGGAGACGGAATTCGC
6	CRISPR sgRNA ADAR1ko_ exon4_R	aaacGCGAATTCCGTCTCCTGTCC
7	non- targeting sgRNA_F	caccGTATTACTGATATTGGT
8	non- targeting sgRNA_R	aaacACCAATATCAGTAATAC
9	A1KO_11_f w	CACCGAGCAAGATGAGTTCCGAGAC

10	A1KO_11_r v	AAACGTCTCGGAACTCATCTTGCTC
11	A1KO_39_f w	CACCGTAGCTGTTGATCCCCTCTG
12	A1KO_39_r v	AAACCAGAGTGGGATCAACAGCTAC
13	W58X_uAg _F	CTGCCCCGTGCCCTAGCCCACCCT
14	W58X_uAg _R	AGGGTGGGCTAGGGCACGGGCAG
15	pENTR_pla sm_F	TTTTTCTAGACCCAGCTTTCTTGTA
16	pENTR_pla sm_R	GGTGTTCGTCCTTTCCACA
17	Oligo_gRN A_W58X	tggaaaggacgaaacaccTCAGGGTGGTGGCCCTGAAAAAGGGCCGAGGGTGGG CCAGGGCACGGGCAGCTTGC GGCCCTGAAAAAGGGCC TGGTGCAGATtt tttctagaccagctt
18	Apob_F	TGCATCCTGGATTCAAAATGTGG
19	eGFP_R	TTGAAGTCGATGCCCTTCAG
20	A1_KO1A_ fw	CATTGATGGCTCTGTGGGTGTTC
21	A1_KO1A_ rv	GCTGAAAAGCACCCAGGGAC
22	A1_KO2A_ fw	GTACCTCTCAGATCCTTTGAGAAGTC

23	A1_KO2A_ rv	GCATGCTGTAACCCTGTAGTTC
24	B2m_fw	CAAGCATCATGATGCTCTGAAG
25	B2m_rv	GTAAAAGTAACAAAAGCAGAAGTAGCC
26	mCherry- mApob- eGFP_SEQ	CTCCCACAACGAGGACTACACC
27	MAVS_F	TACCCTGCCTGGCCTCAAACCTATTA
28	MAVS_R	ACTTCATGCTGTCTGGGAGCAA
29	DDX58_F	ATTTGGCCCTGTTGAGCACTCT
30	DDX58_R	ACGTCCAGGAAACCGCAAACCTA
31	SSR3_F	TGGGCTCCATGCAAGAAGCTTGGAA
32	SSR3_R	GCACTGCCATCTAGTGGCAAGTTT
33	ARSD_reg1 _F	GAGCCTGACTGCGTTGCAAACAAA
34	ARSD_reg1 _R	AAGACGGAGGGGTGAAAACATCG
35	ARSD_reg2 _F	CACCCCTCCGTCTTAAAGCATTGT

36	ARSD_reg2_R	CCCTTGATCGGCTCATTACTTGGGA
37	CTSS_F	CTGGTGATGGGGTTTAGCAACT
38	CTSS_R	TGCCAAATAAAGGCCCTGGTCA
39	Aldoc_F	AAGGGCTATGACCCACTTCCATGT
40	Aldoc_R	CGATTCCAATTCGAGCGATTGAGG
41	Atp6ap2_F	GCTAGACTTAGACAACAGGTTTGG
42	Atp6ap2_R	GTCTACAGATTGAAGCCATACCAC
43	B2m_F	CAAGCATCATGATGCTCTGAAG
44	B2m_R	GTAAAAGTAACAAAAGCAGAAGTAGCC
45	Casp6_F	AACCTAGCAAGTAGGGCCATCTGT
46	Casp6_R	CATGACCAAGTCAAATAGGCCAC
47	Cd36_F	CTGGCTACATCTTTGGTAAAGCCG
48	Cd36_R	GGGCCACCCAGTCATGATAG
49	Rab7_F	TCCGTTCTGAGCAGGCTGTTTTGT

50	Rab7_R	TCTGGTGGGTTCTCCTTTCTCTT
51	Reep5_F	GCCTTGGAAGCTTCCCGCTGTATT
52	Reep5_R	GTCTCCCTTCTCAGGTCACAGGT
53	Serinc1_F	TGTATCGCTGCTGTCCAGCAT
54	Serinc1_R	GGCTGGAACATGAAGATGAACTGC
55	Slc39a10_F	ACTGCGGGAATATACTCCCACTCT
56	Slc39a10_R	GCAAGTATCACCTTGCAGGACCAT
57	ARSD_NG S_F	tcgtcggcagcgtcagatgtgtataagagacagGAGCCTGACTGCGTTGCAAACAAA
58	ARSD_NG S_R	gtctcgtgggctcggagatgtgtataagagacagAAGACGGAGGGGTGAAAACATCG
59	CTSS_NGS _F	tcgtcggcagcgtcagatgtgtataagagacagCTGGTGATGGGGTTTAGCAACT
60	CTSS_NGS _R	gtctcgtgggctcggagatgtgtataagagacagTGCCAAATAAAGGCCCTGGTCA
61	DDX58_N GS_F	tcgtcggcagcgtcagatgtgtataagagacagATTTGGCCCTGTTGAGCACTCT
62	DDX58_N GS_R	gtctcgtgggctcggagatgtgtataagagacagGAGAACAATGGCACACGTTAAGAG
63	MAVS_ NGS_F	tcgtcggcagcgtcagatgtgtataagagacagCCATGAGCCCATCACCCAAC

64	MAVS_ NGS_R	gtctcgtgggctcggagatgtgtataagagacagACTTCATGCTGTCTGGGAGCAA
65	Slc39a10_N GS_F	tcgtcggcagcgtcagatgtgtataagagacagACTGCGGAATATACTCCCCTCT
66	Slc39a10_N GS_R	gtctcgtgggctcggagatgtgtataagagacagGCAAGTATCACCTTGCAGGACCAT
67	Aldoc_NGS _F	tcgtcggcagcgtcagatgtgtataagagacagAAGGGCTATGACCCACTTCCATGT
68	Aldoc_NGS _R	gtctcgtgggctcggagatgtgtataagagacagCGATTCCAATTCGAGCGATTGAGG
69	Atp6ap2_N GS_F	tcgtcggcagcgtcagatgtgtataagagacagGGAGAACGCACTGGGTTTCTTA
70	Atp6ap2_N GS_R	gtctcgtgggctcggagatgtgtataagagacagGTCTACAGATTGAAGCCATAACCAC
71	Serinc1_NG S_F	tcgtcggcagcgtcagatgtgtataagagacagAGGCTCGGGTTAGGCACTAAGATA
72	Serinc1_NG S_R	gtctcgtgggctcggagatgtgtataagagacagGGCTGGAACATGAAGATGAACTGC
73	B2m_NGS_ F	tcgtcggcagcgtcagatgtgtataagagacagcaagcatcatgatGCTCTGAAG
74	B2m_NGS_ R	gtctcgtgggctcggagatgtgtataagagacagGTAAAAGTAACAAAAGCAGAAGTAGC C
75	Rab7_NGS _F	tcgtcggcagcgtcagatgtgtataagagacagTCCGTTCTGAGCAGGCTGTTTTGT
76	Rab7_NGS _R	gtctcgtgggctcggagatgtgtataagagacagTCTGGTGGGTTCTCCTTTCCTCTT

SUPPLEMENTARY FIGURES

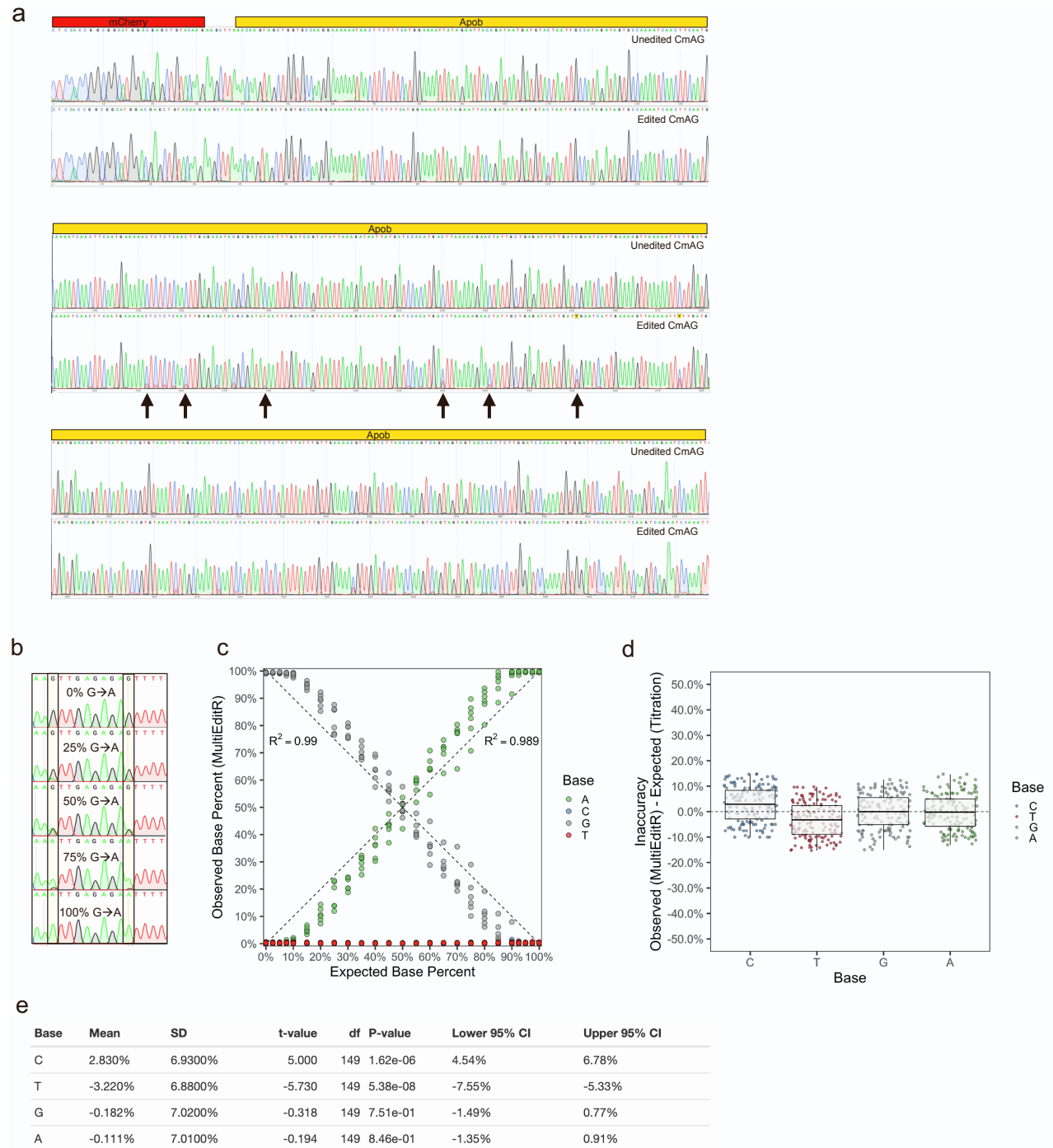


Fig. S1 | C-to-U editing of Apob by APOBEC1 within CmAG plasmid.

a, Sanger sequencing chromatograms from HEK293T cells transfected only with CmAG or with CmAG, APOBEC1 and RBM47. Amplification of Apob region from CmAG transcript and

following Sanger sequencing show abundant C-to-T editing in several sites along the sequenced area. Black arrows point to the 6 Cs which are unedited (C) in pJET-CmAG-WT and edited (T) in the pJET-CmAG-6x (Supplementary materials and Fig. 1a). **b**, Chromatograms from G-to-A titration showing a change in peak height at two sites. **c**, Titration of pJET-CmAG-WT with pJET-CmAG-6x sequenced with the forward primer, coefficient of determination was calculated relative to the identity line $y = x$, $N = 6$ sites per chromatogram. **d**, Inaccuracy of MultiEditR relative to expected titration values, significance was determined using Student's one-sample t-test relative to an inaccuracy of 0%. **e**, Table of results from Student's one-sample t-test of inaccuracies.

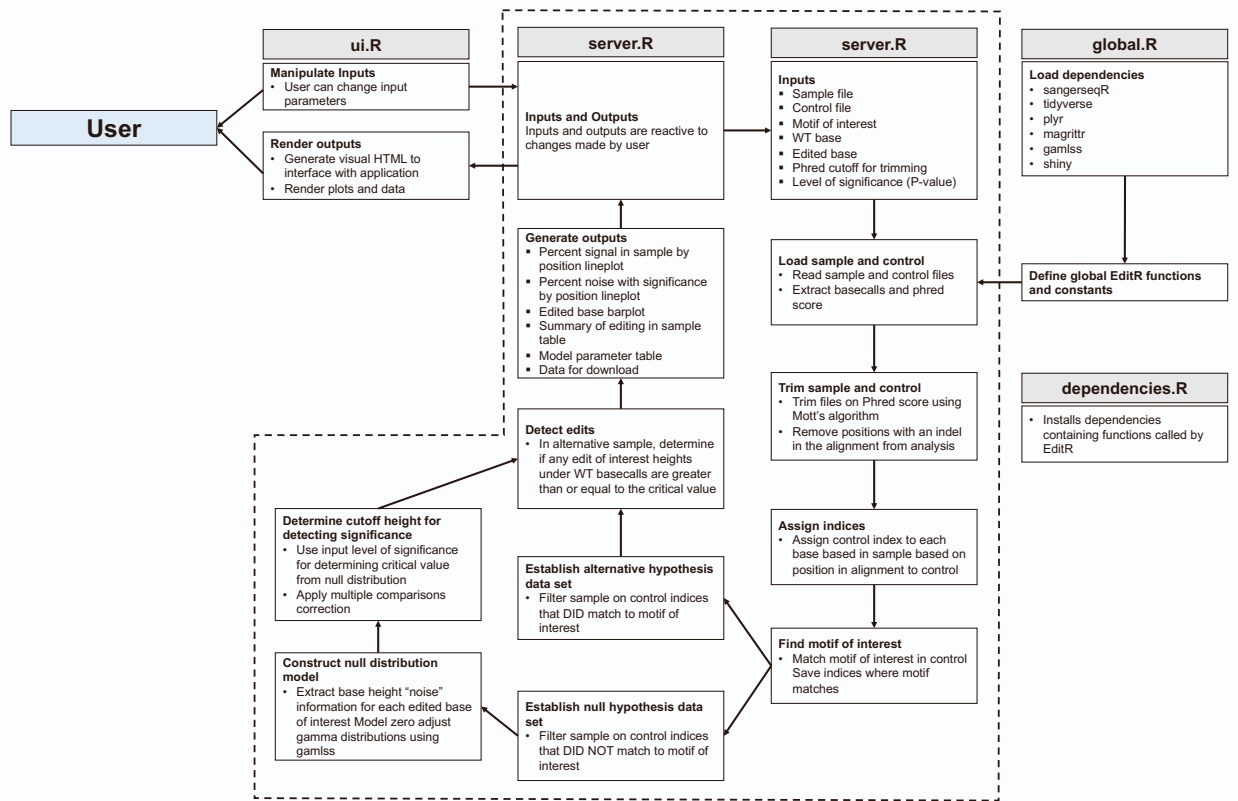


Fig. S2 | MultiEditR algorithm.

MultiEditR algorithm flow chart in the context of the MultiEditR web application made using R Shiny (z.umn.edu/multieditr). Source code available at:

<https://github.com/MoriarityLab/MultiEditR>

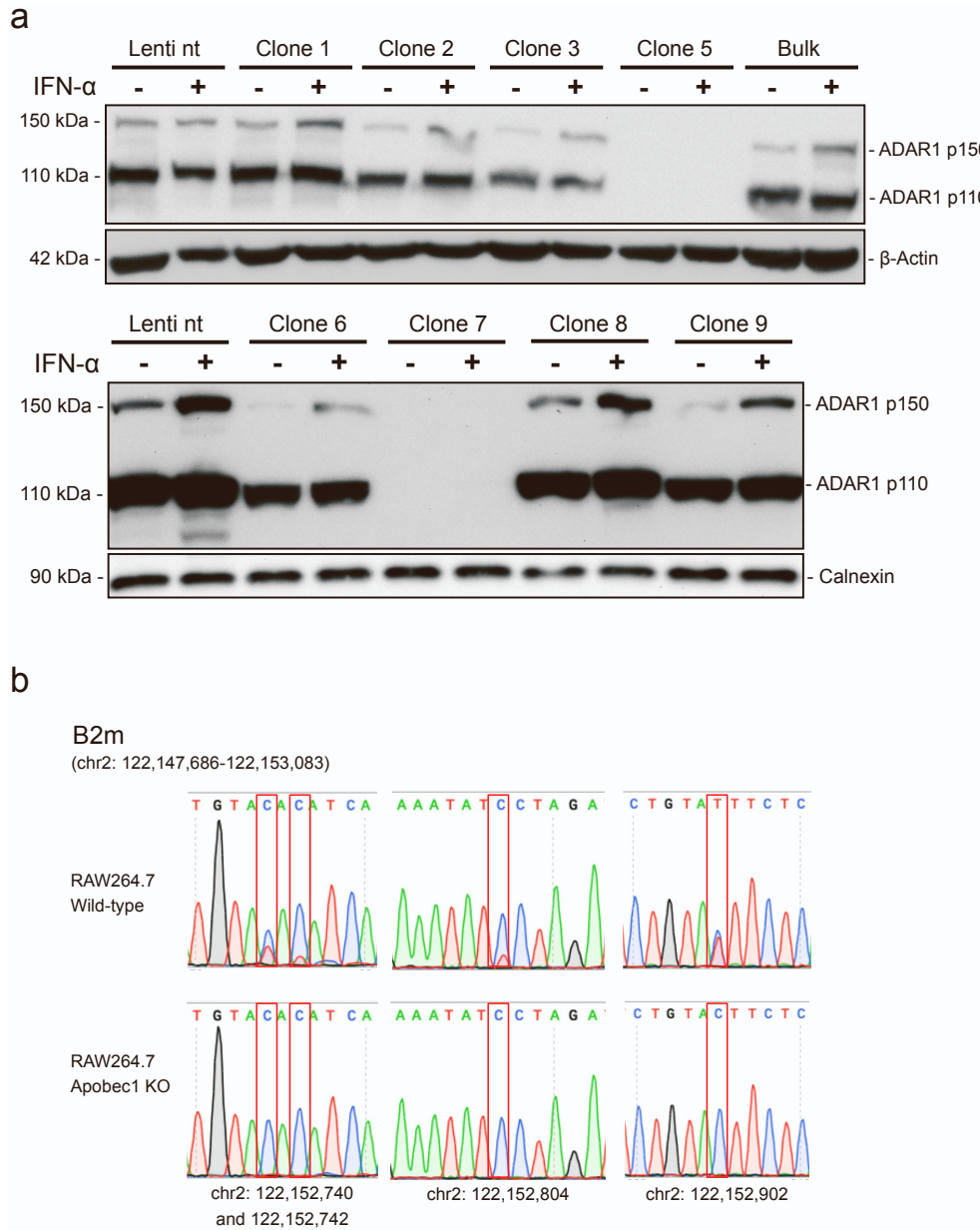


Fig. S3 | Generation of human ADAR1 and murine APOBEC1 KO cell lines.

a, Western blot of A549 KO clones and bulk, after transduction with lenti-CRISPR-ADAR1 exon 4. A549 cells were stimulated with 200 U/ml of IFN- α (pbl assay science, cat. no.#11100-1) for 16 h to evaluate the presence of ADAR1 p150. “Lenti nt” is the non-targeting control and was generated by transducing cells with the same vector (LentiCRISPRv2) but containing a non-targeting sgRNA (see Supplementary Table 3). β -Actin and Calnexin were used as loading controls

(Mouse β -Actin monoclonal antibody, Sigma-Aldrich, cat. no.#A5441; Rabbit Calnexin polyclonal antibody, Enzo Life science, cat. no.#ADI-SPA-865-F). **b**, Sanger sequencing chromatograms for RAW 264.7 wild-type and APOBEC1 knock-out after RT-PCR amplification of B2m 3'UTR region (oligos #24-25). The complete absence of C-to-U editing along the sequenced region confirms the deficiency of APOBEC1 editing activity within the knock-out clone.

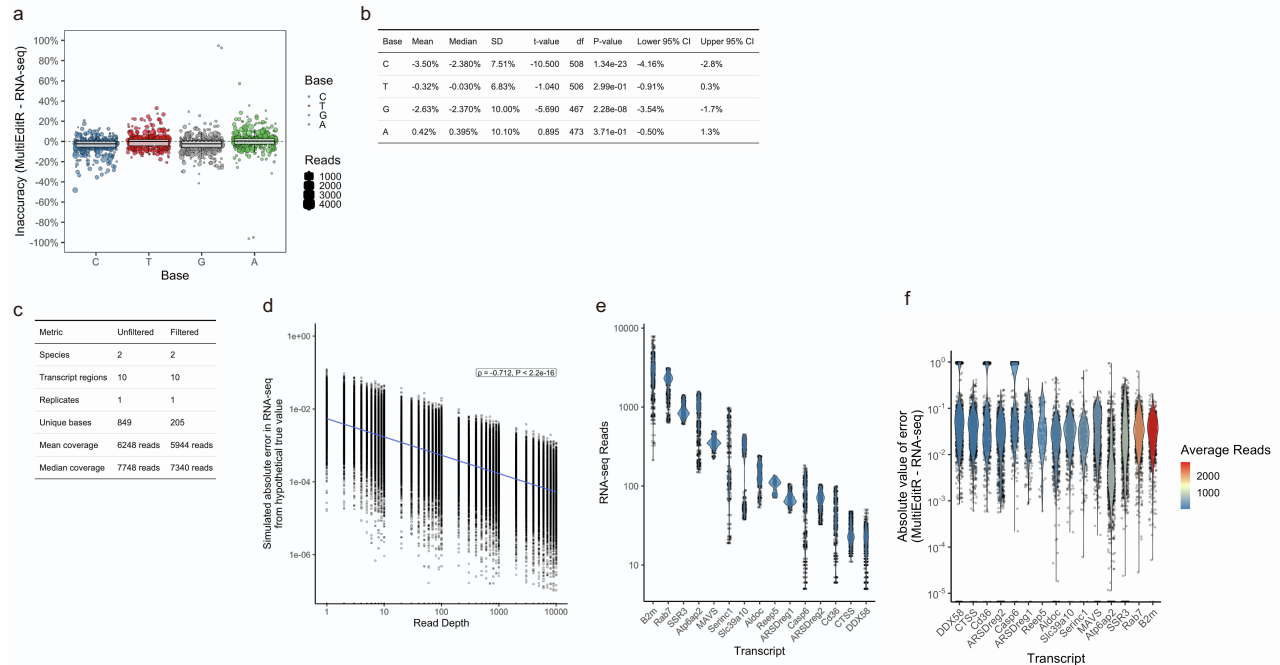


Fig. S4 | Descriptive statistics, coverage and error of samples in RNA-seq data set.

a-b, Comparison of MultiEditR to RNA-seq measurements. All data is filtered on between 1% and 99% editing measured by either method. Coefficients of determination represent regression to the identity line. Dot size is proportional to read coverage at the base of interest in RNA-seq. Tables represent results of Student's pairwise t-test between measurement methods. **c**, Descriptive statistics of samples in RNA-seq data set. **d**, Simulation of expected absolute error in RNA-seq editing value from true editing value as a function of read depth. Absolute error of editing measurement is negatively correlated with read depth (Spearman's correlation coefficient, $\rho = -0.712, P < 2.2e-16$). **e**, Violin plots of read depth at each base for each transcript analyzed. **f**, Violin plots of absolute value of error in MultiEditR editing measurement minus REDIttools RNA-seq editing measurement by each transcript. Plots are colored by average read depth.

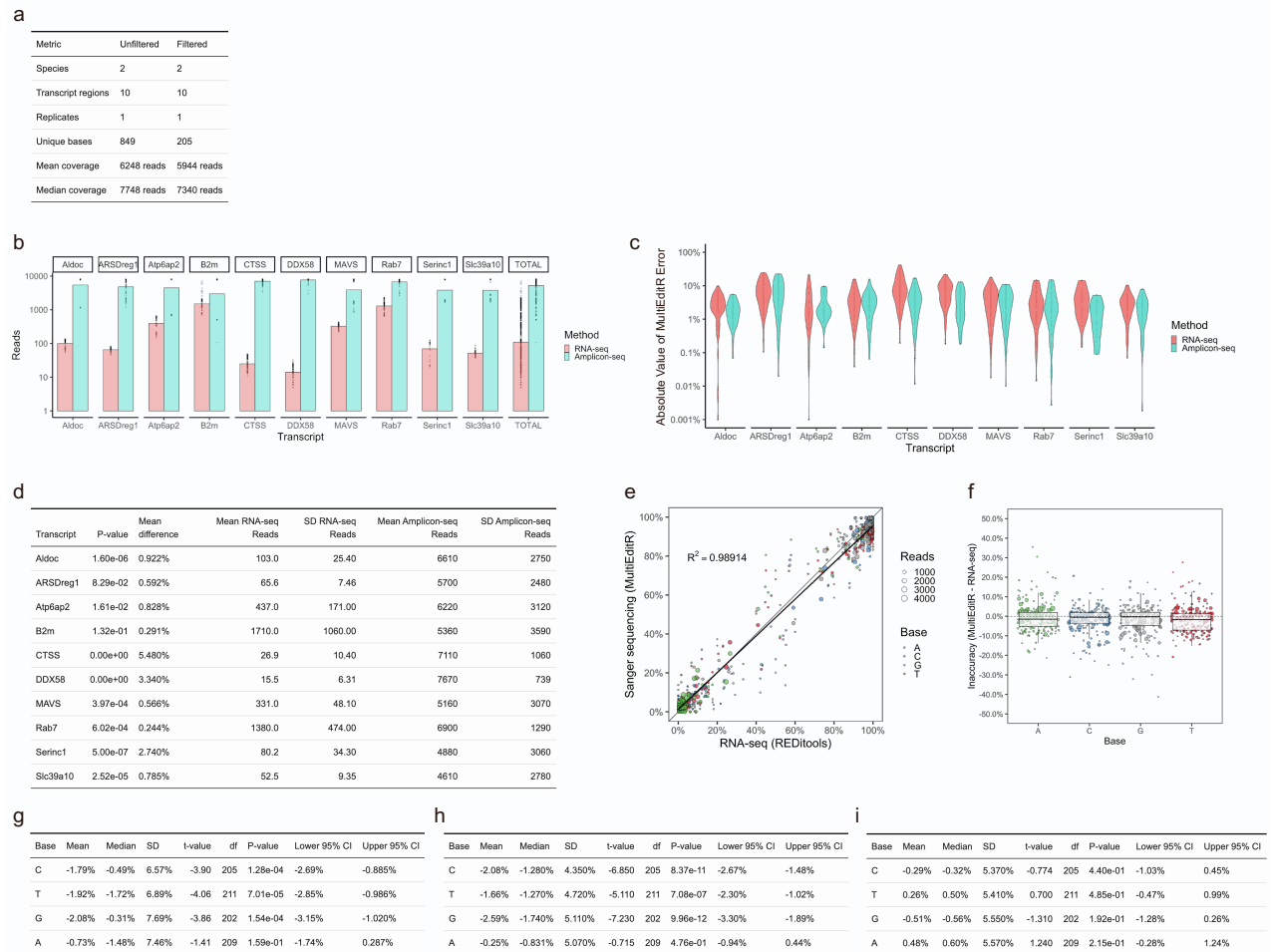


Fig. S5 | Descriptive statistics, coverage and error of samples in the combined RNA-seq and Amplicon-seq data set.

a, Descriptive statistics of samples in the combined data set. **b**, Barplots of read depth in each sample for RNA-seq and Amplicon-seq data for each transcript. Amplicon-seq read depth is higher for every transcript. **c**, Violin plots of absolute value of error in MultiEditR editing measurements minus REDIttools RNA-seq or Amplicon-seq editing measurements. **d**, Table comparison of RNA-seq to Amplicon-seq editing values for each transcript. **e-f**, Comparison of MultiEditR to RNA-seq measurements. Data is filtered on between 1% and 99% editing measured by Amplicon-seq. Coefficients of determination represent regression to the identity line. Dot size is proportional to read coverage at the base of interest in RNA-seq. **g**, Tables of Student's pairwise t-test results

between MultiEditR and RNA-seq. **h**, Tables of Student's pairwise t-test results between MultiEditR and Amplicon-seq. **i**, Tables of Student's pairwise t-test results between RNA-seq and Amplicon-seq.

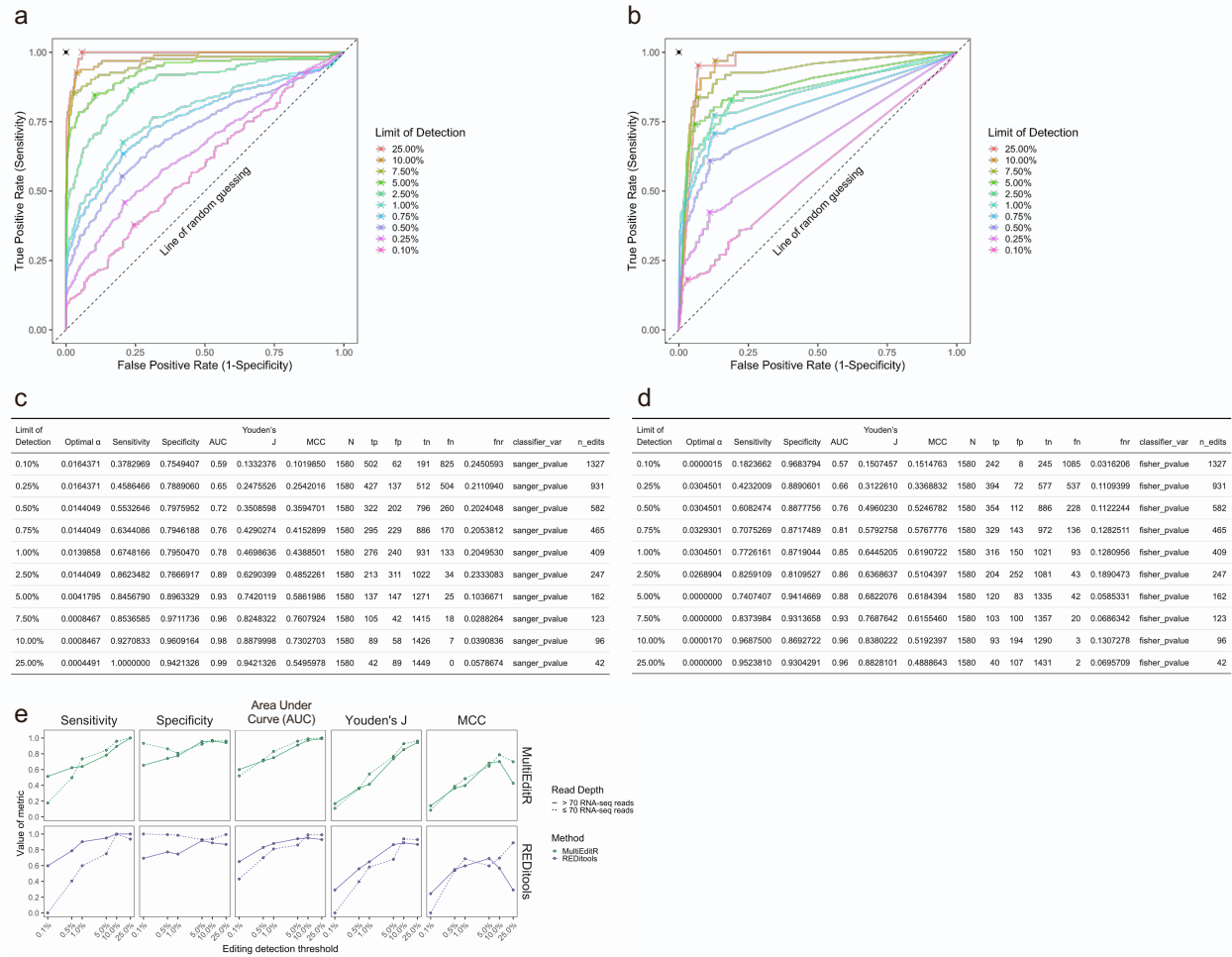


Fig. S6 | Receiver Operating Characteristics (ROC) analysis of MultiEditR and REDIttools RNA-seq, compared to REDIttools Amplicon-seq.

a, MultiEditR ROC across different limits of detection. Hashed points represent optimal cutpoint.

b, REDIttools RNA-seq ROC across different limits of detection. Hashed points represent optimal cutpoint.

c, MultiEditR ROC analysis parameter table across levels of detection. **d**, REDIttools RNA-seq ROC analysis parameter table across levels of detection.

e, Lineplots for ROC parameters for MultiEditR and REDIttools across limits of detection, broken up by regions that had high RNA seq coverage (>70 reads), and low RNA-seq coverage (≤ 70 reads). MultiEditR is more robust in regions that have poor coverage in RNA-seq.

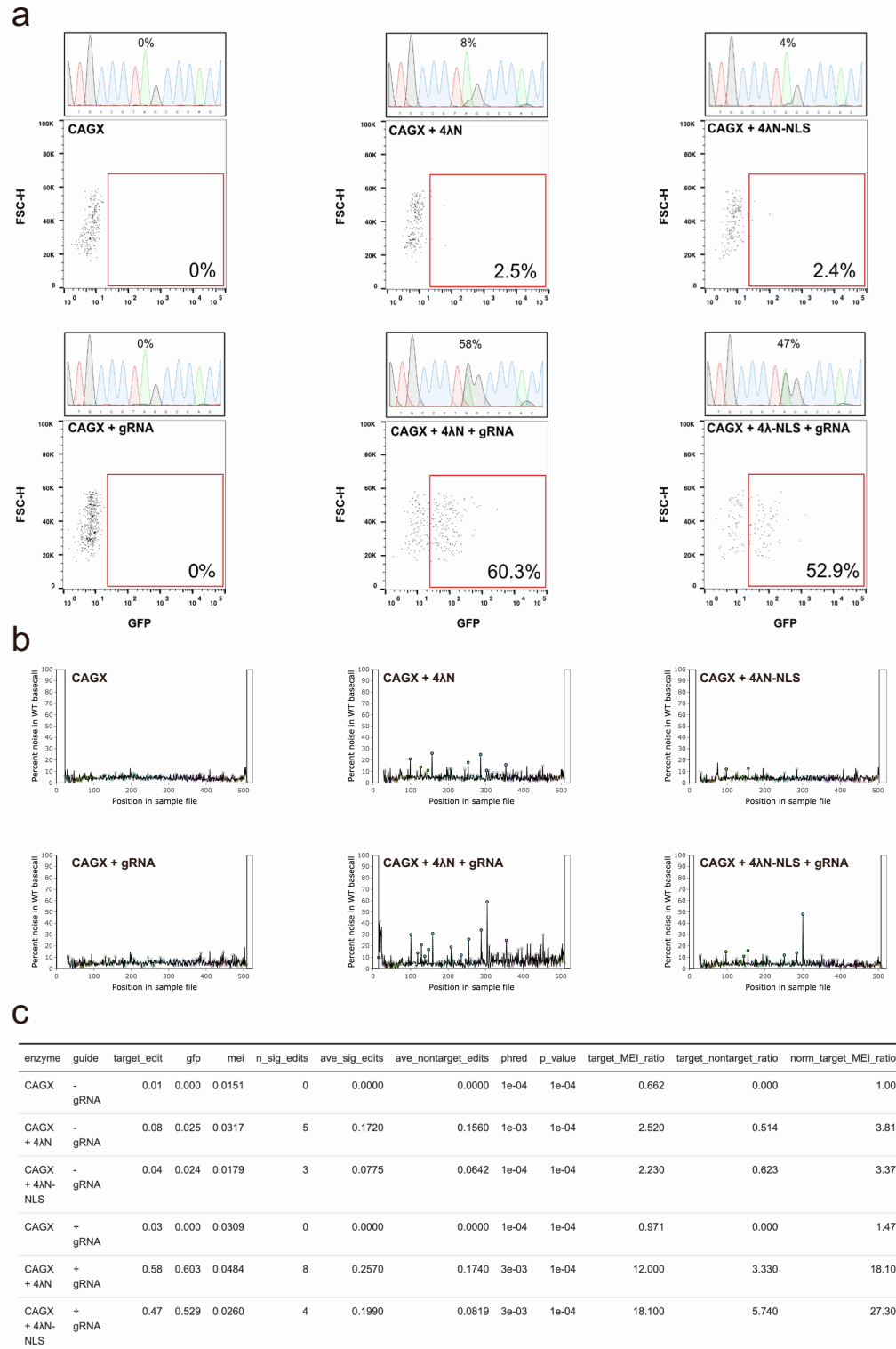


Fig. S7 | Reactivation of eGFP by RNA targeted editing.

a, FACS analysis for GFP positive cells after transfection with 4λN and 4λN-NLS in presence and absence of the gRNA to re-activate eGFP by RNA base-editing. The percentage in the plot represents the GFP+ cells of the mCherry+ cells detected by FACS. Above each FACS plot, it is shown A-to-G editing at position W58X for that sample; the percentage of editing is calculated by MultiEditR. **b**, Plots generated in MultiEditR showing the distribution of A-to-G editing along the sequenced region. From this plot appears evident that 4λN has a higher editing activity which leads to a more prominent RNA off-target effect both in presence and absence of the gRNA. **c**, MultiEditR parameters used in this analysis.